Observation of Intermittent Chaos Caused by Delayed Feedback in a Laboratory Plasma

Takao FUKUYAMA and Yutaro SUEYOSHI

Faculty of Education, Nagasaki University, 1-14 Bunkyo-machi, Nagasaki 852-8521, Japan

(Received 18 August 2023 / Accepted 26 October 2023)

In this study, experimental investigation was conducted on intermittent chaos caused by time-delayed feedback in the laboratory plasma. In a limit cycle with time-delayed feedback, a periodic system moved down the intermittency route to chaos, with the appearance of an increasing number of bursts that interfered with the laminar flow, as the feedback signal strength increased if an appropriate delay time was not selected. Analyses of the obtained time series revealed that the system with feedback has chaotic characteristics and that the shape of the recurrence plot differs from that of the turbulent state in which feedback is not applied. By observing the spatiotemporal structure, it was revealed that the system, which is in a periodic state both in time and space, transitions to a state of spatiotemporal chaos through the application of feedback. In this study, it was observed that the system undergoes intermittency, which leads to a chaotic state when time-delayed feedback is provided to nonlinear limit-cycle oscillations.

Keywords: chaos, limit-cycle, intermittency, controlling chaos, delayed feedback, ionization wave

DOI: 10.1585/pfr.18.1401088

1. Introduction

For over half a century, chaos [1–9] has been extensively studied, particularly in the field of plasma physics. Routes to chaos through intermittency [8] have been extensively studied from both theoretical and experimental perspectives, in addition to routes to chaos through period-doubling bifurcations [10] and quasi-periodicity [11]. Chaos control and synchronization of coupled nonlinear oscillators are popular topics in nonlinear physics [12–25]. The time-delayed auto-synchronization method [15], a control method for chaos, has been widely used in experimental systems [18] because it is versatile and noise resistant. The chaos control method is based on chaotic oscillation synchronization. Chaotic control is typically achieved by incorporating a feedback circuit into a chaotic system.

Prior studies [5, 26] indicated that an appropriate time delay and amplification rate must be selected to achieve control; otherwise, the original chaotic system will be further disturbed. Furthermore, as typical nonlinear phenomena, nonlinear periodic oscillations (limit cycles) and chaos were observed. Therefore, this study investigates the dynamic behavior of limit cycle oscillations when time-delay feedback is used. Similar to previous studies, time-delayed feedback methods were used to control chaotic states. The basic concept of the chaos control method involves pulling an orbit into a periodic orbit embedded in a chaotic orbit. The chaotic system is further disturbed if appropriate parameters in the time-delayed feedback for chaos control are not selected; however, the mechanism underlying this disturbance remains unclear. In this study, we identified that, when time-delayed feedback with inappropriate parameters is applied to a limit cycle, which is a periodic orbit, the limit cycle collapses, leading to chaos. Therefore, we consider that the further disruption of chaotic orbits by the application of time-delayed feedback was caused by the collapse of periodic orbits embedded in the chaotic orbit. Thus, we believe that by using the time-delayed feedback method to an ordered state, we can gain insight into chaos control through studies in which the ordered state is disrupted into a chaotic state.

This study investigated the dynamic behavior caused by applying time-delayed feedback to nonlinear limit-cycle oscillations in laboratory plasma. The remainder of this paper is organized as follows: Sec. 2 describes the experimental setup and configuration of the laboratory plasma. Section 3 presents the results and discusses the appearance of intermittent chaos using time-delayed feedback to the limit cycle. Finally, Sec. 4 summarizes the study.

2. Experimental Setup and Configuration

The experimental setup for the laboratory plasma and a photograph of the generated plasma (captured using a high-speed camera) are shown in Fig. 1. The lower left and right figures in Fig. 1 show the power and wavelength spectra, respectively. The time series of the ionization wave exhibits a quasiperiodic state, and the phase velocity of the

author's e-mail: fukuyama-takao@nagasaki-u.ac.jp

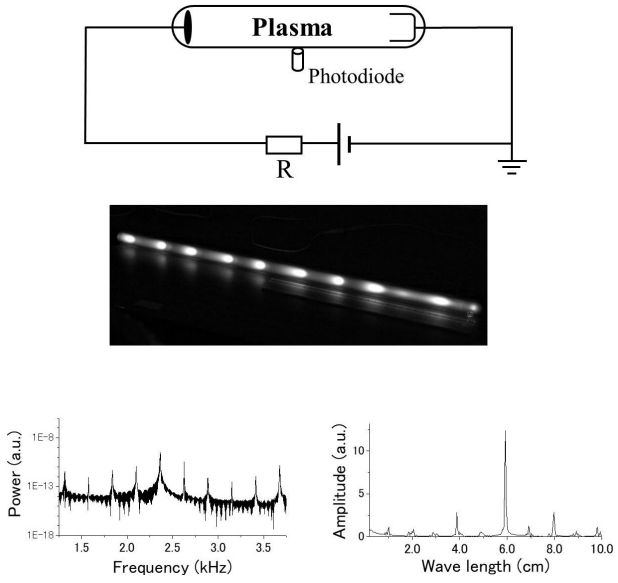

Fig. 1 Experimental setup for a laboratory plasma and photograph of generated plasma (captured with a high-speed camera). Additionally, the lower left and right figures show the power and wavelength spectrums, respectively. A glass tube with a length of 75.0 cm and a diameter of 2.0 cm is used. Ne gas is introduced and confined at a pressure of approximately 478 Pa. Ne plasma is produced under the condition of DC glow discharge between two electrodes placed 60.0 cm apart.

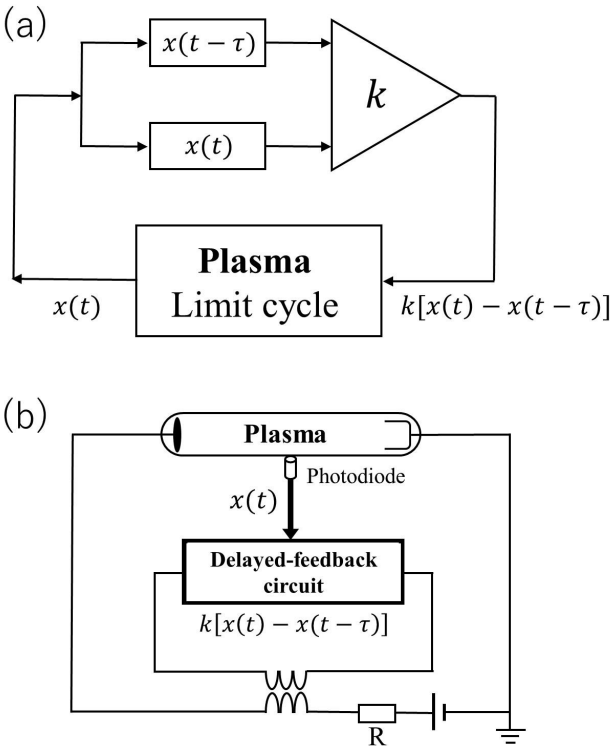

Fig. 2 Schematic of the circuit based on the time-delayed autosynchronization method: (a) how the feedback is calculated and (b) how it is integrated into the system. Time series data are collected by a photodiode placed 30 cm from the anode. Time series data are obtained at a sampling rate of 0.01 ms. The feedback signal $F(t)$ is constructed based on a signal calculated from the difference between the delayed output signal $x(t-\tau)$ and output signal $x(t)$. The feedback signal $F(t)$ applied to the system of ionized waves is adjusted proportionally to the difference of two values, an arbitrary variable $x(t)$ and a time-delayed variable $x(t-\tau)$. τ and k denote the delay time and proportionality constant, respectively. τ is fixed at a 0.625 period with respect to the fundamental period of the system.

fundamental wave was approximately 140 m/s. The equipment used in the experiments was largely identical to that used in previous studies [25, 26]. The experiments were performed using a glass tube with a length of 75.0 cm and a diameter of 2.0 cm. Following a high vacuum evacuation of the glass tube, Ne gas was introduced and confined in the tube at a pressure of approximately 478 Pa. The Ne plasma was produced and maintained under the condition of glow discharge between a pair of electrodes placed 60.0 cm apart when a high DC electric field was generated using a regulated DC power source (HV1.5-0.3, TAKASAGO). Owing to the ionization instability, when a high DC voltage is applied between the electrodes, an ionization wave is excited in the Ne plasma. Ionization waves are self-excited, unstable phenomena caused by ionized collisions with spatial degrees of freedom. The typical electron and ion temperatures were approximately 10 and 0.025 eV, respectively. The discharge current is an important system-governing parameter.

Photodiodes (S6775, HAMAMATSU), a digital oscilloscope (GDS-1072A-U, GWINSTEK), and a line-scan camera (TL-4096ACL, TAKENAKA) were used to sample fluctuations in light emission from the plasma as time-series signals. The LabVIEW system (NI 2020) was used to perform arithmetic operations on the resulting time series data and output the processed data. A transformer (EF-4N, SHIMADZU) and an amplifier (4015, NF ELECTRONIC INSTRUMENTS) were used to amplify the feedback signal. A series of experiments focused on ionization waves [18, 27–33] in a positive column produced by glow discharge in Ne plasma. The plasma state is maintained by the propagation of ionization wavefronts, referred to as ionization waves, through a vacuum tube.

The feedback of the discharge current through the external discharge circuit causes nonlinearity in the ionization wave. The propagation of the ionization wave in a vacuum tube results in the reconnection of the wavenumber near the cathode, resulting in the chaotic behavior of the ionization wave. The ionization waves in laboratory plasma exhibit a wide variety of nonlinear phenomena, such as chaos and nonlinear limit cycles, rendering them suitable for studying nonlinear phenomena. The oscillation of the ionization wave was governed by varying the intensity of the discharge current as a control parameter. Dynamic behavior can be observed as a time series of fluc-

tuations in the emission intensity, revealing that the system exhibits different types of dynamic behavior, such as chaotic and periodic states. In the experiments, the DC discharge current and voltage were set at 21.2 mA and 615 V, respectively. At this discharge current, the system exhibited periodic limit-cycle oscillations.

Figure 2 shows a schematic of the circuit based on the time-delayed auto-synchronization method. Figures 2 (a) and 2 (b) show how the feedback was calculated and integrated into the system. Time-series data were collected using a photodiode placed 30 cm away from the anode. Time-series data were obtained at a sampling rate of 0.01 ms. The feedback signal was constructed based on a signal calculated from the difference between the delayed output signal $x(t-\tau)$ and output signal $x(t)$. The feedback signal $F(t)$ applied to the system of ionized waves was adjusted in proportion to the difference between two values: an arbitrary variable $x(t)$ and a time-delayed variable $x(t-\tau)$.

$$F(t) = k[x(t) - x(t-\tau)], \tag{1}$$

where τ and k represent the delay time and proportionality constant, respectively, corresponding to the feedback amplification factors. In this study, τ is fixed at 0.625, corresponding to 0.252 ms, which is a 0.625 period of the fundamental frequency of 2.478 kHz.

3. Results and Discussion

Figure 3 shows the time series corresponding to increasing values of k for (a) $k = 0$ (before feedback was applied), (b) $k = 9$ (threshold for the appearance of intermittent chaos), (c) $k = 16$, (d) $k = 18$, (e) $k = 20$, and (f) $k = 23$. As shown in Fig. 3, as k increases, the number of burst states that interfere as the laminar state increases and the system transforms into a chaotic state. A video of each state can be observed in [34], corresponding to Fig. 3. The peak-to-peak voltages, as the feedback signal intensity, were measured as follows: for $k = 9$, approximately 5 V (approximately 0.8% of the discharge voltage of 615 V); for $k = 16$, approximately 9 V (approximately 1.5% of one voltage); and for $k = 23$, approximately 13 V (approximately 2.1% of one voltage). The interval between bursts was defined as laminar. The characteristics of intermittent chaos observed in this study are that the farther away from the threshold of intermittent occurrence, the shorter the interval between bursts, and the more chaotic it becomes.

Figure 4 shows $\langle T_L \rangle$ with respect to $k - k_c$, where $\langle T_L \rangle$ indicates the average value of the laminar duration for the value of k, and k_c indicates the threshold value k for intermittent chaos appearance; in this study, $k_c = 9$. The error bars represent the standard deviation, which was calculated for more than 50 measurements for each value of k. Notably, for the range of parameters where k slightly exceeds the threshold value k_c, the laminar duration is extremely long, and measurement was not possible owing to technical problems. The experimental results in Fig. 4 show that as k increases, $\langle T_L \rangle$ becomes shorter, that is, bursts appear more frequently in laminar flow, and the system becomes more turbulent and chaotic.

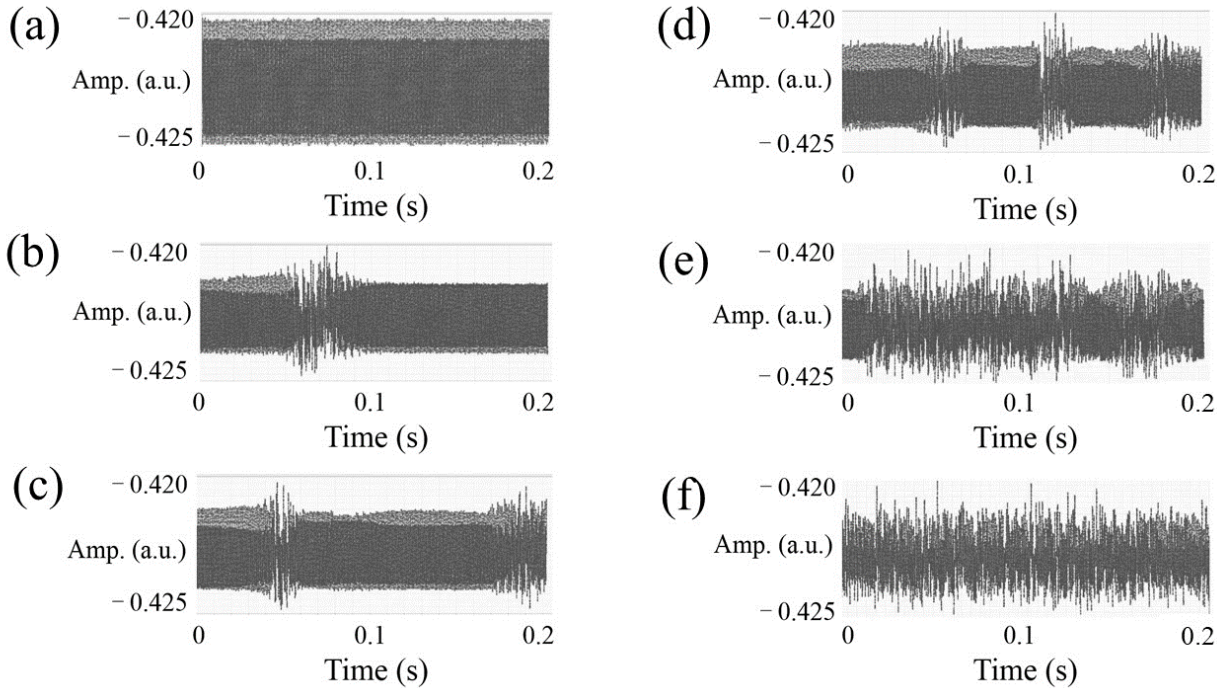

Fig. 3 Time series corresponding to increasing values of k: (a) $k = 0$ (before feedback is applied), (b) $k = 9$ (threshold for intermittent chaos appearance), (c) $k = 16$, (d) $k = 18$, (e) $k = 20$, and (f) $k = 23$. Movie of each state is available in the Ref. [34].

In addition to the quantitative measurements shown in Fig. 4, Fig. 5 presents a recurrence plot for each time series for visual examination. In Fig. 5, the difference DIF_ij between points X_i and X_j of the time-series data to be analyzed is visualized as a gradation at the coordinates (i, j) of a two-dimensional plane. The smaller the DIF_ij (stronger correlation), the darker the gradient; the larger the DIF_ij (weaker correlation), the lighter the gradient. In Fig. 5 (a), $k = 0$, which indicates that the system is in a laminar state with a periodic structure. In Fig. 5 (b), $k = 9$, which is the threshold for the occurrence of intermittency, and the appearance of burst is confirmed in the periodic structure. In Fig. 5 (c), $k = 16$, which indicates an increase in the appearance of burst. In Fig. 5 (d), $k = 20$, which corresponds to a further increase in the appearance of burst, making the entire structure chaotic.

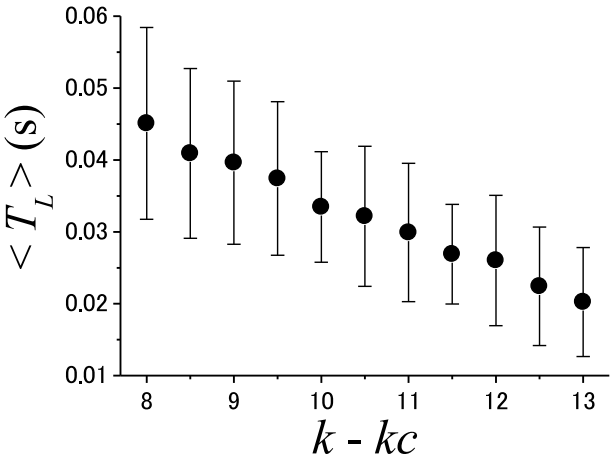

Fig. 4 $\langle T_L \rangle$ with respect to $k - k_c$, where $\langle T_L \rangle$ indicates the average value of the laminar duration for the value of k, and k_c indicates the threshold value k for intermittent chaos appearance. Error bars represent the standard deviation.

Figure 6 shows the power spectrum; Fig. 6 (a) is more chaotic ($k = 23$) when the feedback intensity is sufficiently large. Figure 6 (b) shows turbulent ionization waves without time-delayed feedback (discharge current of 30.0 mA). In Fig. 6, the region between 1 and 3 kHz is focused on and discussed. Figure 6 (a) clearly shows a stronger peak than Fig. 6 (b), indicating that periodicity still exists. This may be because Fig. 6 (a) shows a chaotic system caused by burst filling in the periodic state with time-delayed feed-

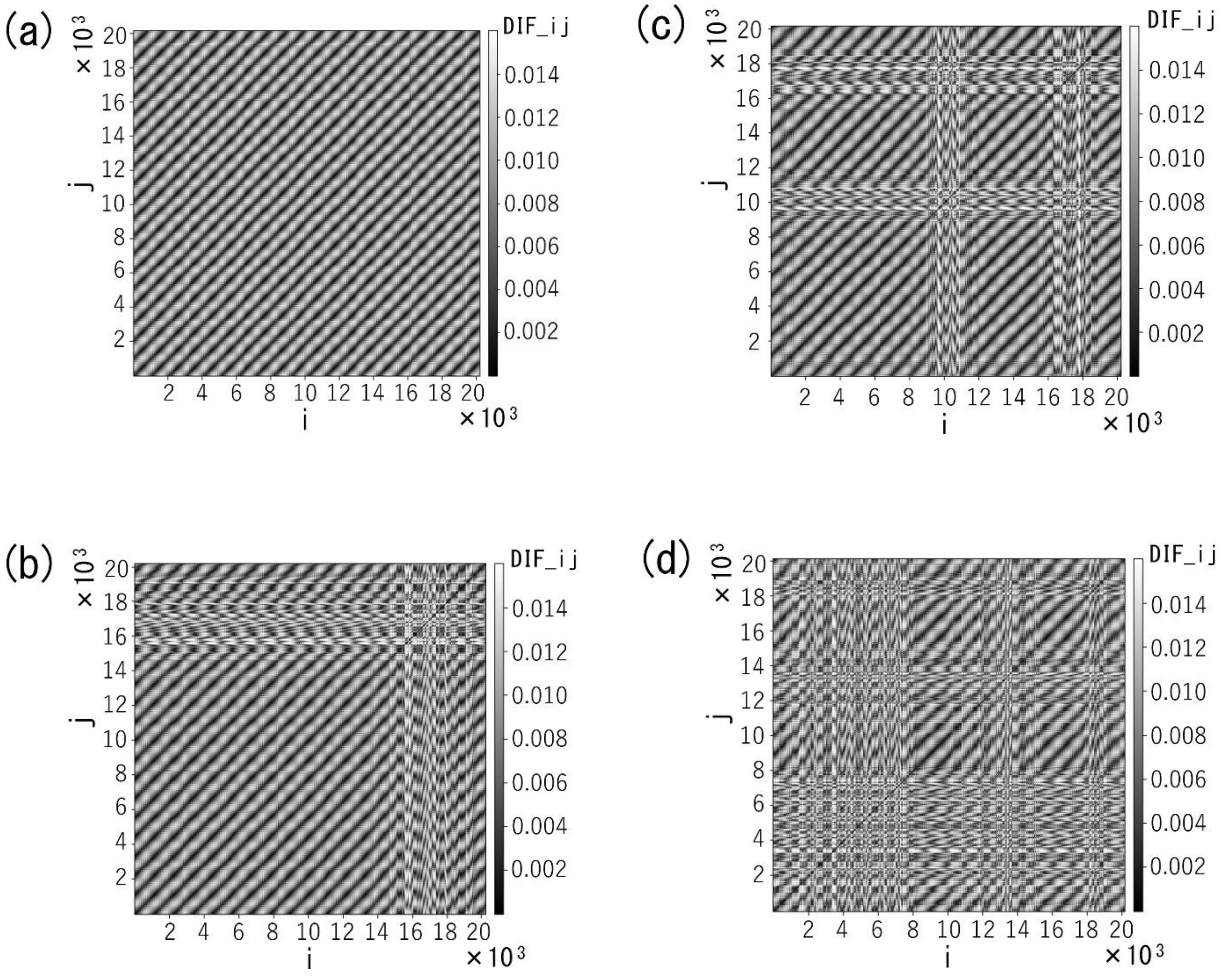

Fig. 5 Recurrence plots for each time series. In cases of (a) $k = 0$, (b) $k = 9$, (c) $k = 16$, (d) $k = 20$. The difference DIF_ij between points X_i and X_j of the time series data to be analyzed is visualized as a gradation at the coordinates (i, j) of a two-dimensional plane.

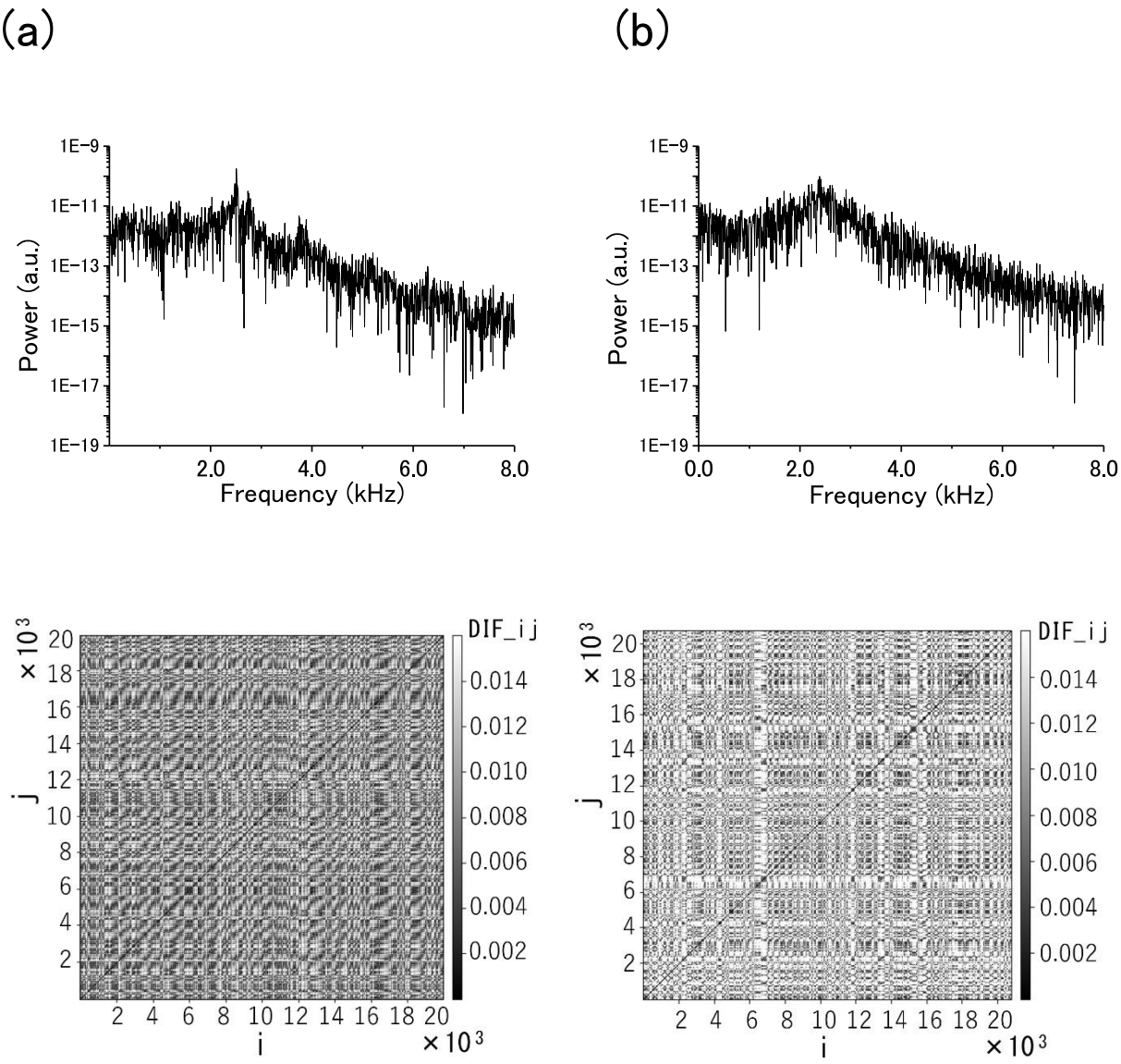

Fig. 6 Power spectra: (a) more chaotic (k = 23) when the feedback intensity is sufficiently large, (b) the turbulent ionization waves without time-delayed feedback (discharge current of 30.0 mA). Additionally, recurrence plots are provided at the bottom of each power spectrum plot.

back, whereas Fig. 6 (b) shows a disordered system from the beginning. An additional discussion will be presented with respect to Fig. 6 using the recurrence plot, which has been added at the bottom of each power spectrum plot. By comparing Fig. 6 (a) and 6 (b), it is clear that their gradations are different. Figure 6 (a) shows a dense overlap of dark areas and the correlation is still present in the time series, whereas Fig. 6 (b) shows many thin areas and little correlation in the time series (close to the turbulence). This is consistent with the aforementioned discussion of the power spectrum.

An analysis is performed using Poincaré sections. To create the Poincaré sections, a reconstructed trajectory embedded in three-dimensional space is created based on a previous study [35]. The parameters are as follows: k = 16, fundamental frequency, 2.46 kHz (0.41 ms), and delay for embedding, 0.07 ms (0.17 period of the fundamental frequency). Figure 7 shows the Poincaré sections when the reconstructed orbit is cut at various angles. The figure of Poincaré sections shows the mechanism through which chaos folds and stretches (i.e., the sensitivity to the initial conditions causes the two points to rapidly move apart and then come close again), which is a characteristic of chaos.

Figure 8 shows the spatiotemporal structure observed using a line-scan camera (a) before (k = 0) and (b) after the feedback application (k = 23). Spatial and time-series signals were sampled every 0.2 mm and 35.0 μs, respectively. These were measured as fluctuations in the intensity of the light emission from the Ne plasma. The light intensity was converted into an 8-bit value, and light emission was measured directly without interference filters. As shown in Fig. 8, the system, which was in a periodic state both in

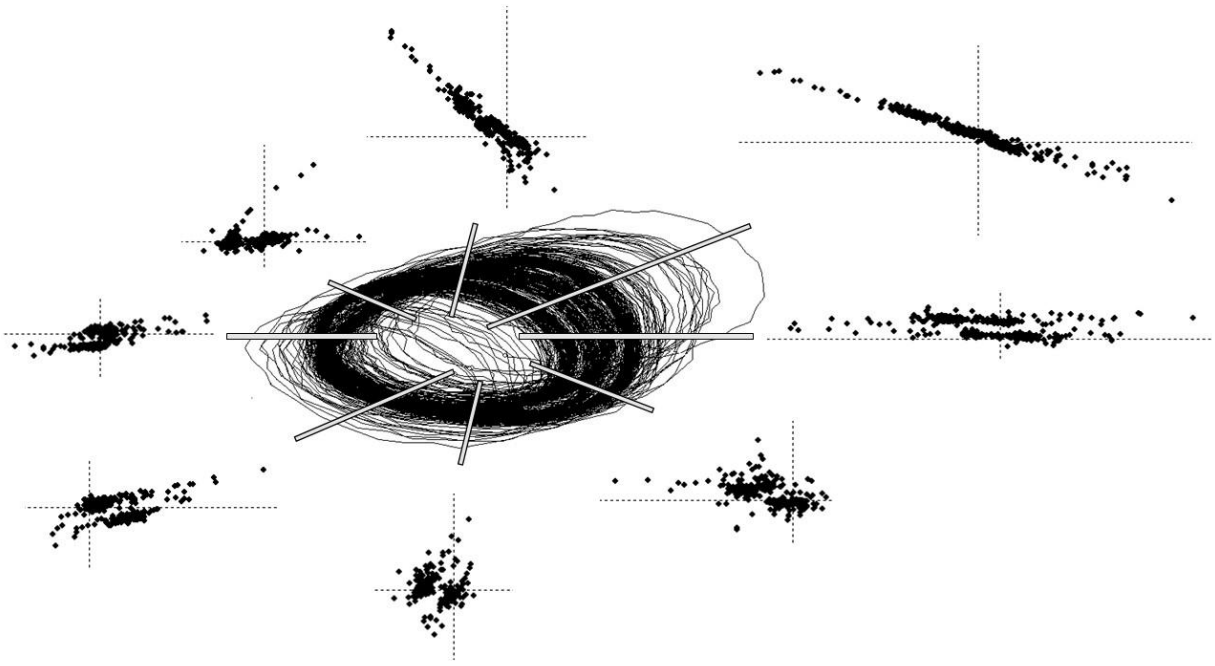

Fig. 7 Poincaré sections when the reconstructed orbit is cut at various angles. The parameters are as follows: $k = 16$, fundamental frequency = 2.46 kHz (0.41 ms), and delay for embedding = 0.07 ms (0.17 period of the fundamental frequency).

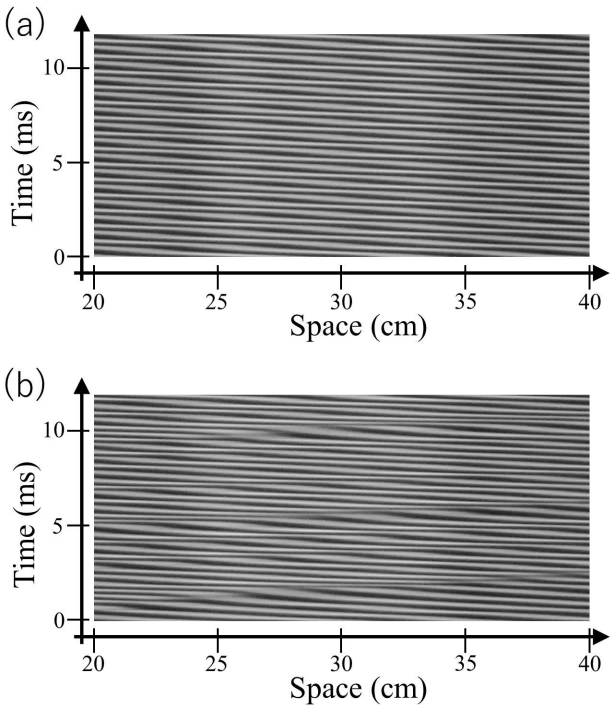

Fig. 8 Spatiotemporal structure observed using a line-scan camera: (a) before ($k = 0$) and (b) after the application of feedback ($k = 23$). Spatial and time series signals are sampled every 0.2 mm and 35.0 μs, respectively. They are measured as fluctuations in the intensity of the light emission from Ne plasma. The light intensity is converted to an 8-bit value. The light emission is measured directly without interference filters.

time and space before feedback was applied, transitioned to a state of spatiotemporal chaos that was disrupted not only in time but also in space by the application of feedback to excite chaos.

4. Conclusion

This study experimentally investigated the dynamic behavior of ionization waves in a laboratory plasma as a nonlinear medium by applying time-delayed feedback to limit cycle oscillations. As the intensity of the amplification rate of the feedback increased, the bursts that interfered with the laminar state gradually increased, leading the system to a chaotic state. This was discussed quantitatively by plotting a graph between the amplification rate and the average value of the laminar duration. This was confirmed experimentally by introducing a recurrence plot and composing Poincaré sections. The power spectrum and recurrence plot due to the application of time-delayed feedback differed from those of the turbulent state without feedback. Furthermore, by observing over time and space, the transition from an ordered state in both time and space before the application of feedback to a state of spatiotemporal chaos by the application of feedback was observed.

This study claims that, in time-delayed feedback control, if an appropriate delay time is not chosen, the system of limit-cycle oscillation goes through intermittency and leads to a chaotic state. Future work will include a classification of the types of intermittent chaos observed in this study based on the theoretical background.

Acknowledgments

The authors are grateful to Dr. K. Terasaka and Dr. Y. Kosuga from Kyushu University for their fruitful discussions and to Mr. N. Nishida and Mr. K. Noguchi from Nagasaki University for their technical assistance. The authors would like to thank Editage (www.editage.jp) for the English language editing. This study was supported by the JSPS KAKENHI (grant numbers 20K03895 and 23K03355).

[1] P. Manneville and Y. Pomeau, Phys. Lett. A **75**, 1 (1979).
[2] W. Boswell, Plasma Phys. Control. Fusion **27**, 405 (1985).
[3] M. Ohno, M. Tanaka, A. Komori and Y. Kawai, J. Phys. Soc. Jpn. **58**, 28 (1989).
[4] D.L. Feng, J. Zheng, W. Huang, C.X. Yu and W.X. Ding, Phys. Rev. E **54**, 2839 (1996).
[5] T. Fukuyama, H. Shirahama and Y. Kawai, Phys. Plasmas **9**, 4525 (2002).
[6] T. Tsubone, T. Saito and N. Inaba, Prog. Theor. Exp. Phys. **2016**, 053A01 (2016).
[7] Y. Nariyuki, M. Sasaki, N. Kasuya, T. Hada and M. Yagi, Prog. Theor. Exp. Phys. **2017**, 033J01 (2017).
[8] K. Okubo and K. Umeno, Prog. Theor. Exp. Phys. **2018**, 103A01 (2018).
[9] T. Fukuyama, R. Yamaguchi and H. Kanzaki, Plasma Fusion Res. **15**, 2401049 (2020).
[10] M.J. Feigenbaum, J. Stat. Phys. **19**, 25 (1978).
[11] S. Ostlund, D. Rand, J. Sethna and E. Siggia, Physica D **8**, 303 (1983).
[12] H. Fujisaka and T. Yamada, Prog. Theor. Phys. **69**, 32 (1983).
[13] L.M. Pecora and T.L. Carroll, Phys. Rev. Lett. **64**, 821 (1990).
[14] E. Ott, C. Grebogi and J.A. Yorke, Phys. Rev. Lett. **64**, 1196 (1990).
[15] K. Pyragas, Phys. Lett. A **170**, 421 (1992).
[16] S. Bielawski, D. Derozier and P. Glorieux, Phys. Rev. E **49**, R971 (1994).
[17] W.X. Ding, H.Q. She, W. Huang and C.X. Yu, Phys. Rev. Lett. **72**, 96 (1994).
[18] Th. Pierre, G. Bonhomme and A. Atipo, Phys. Rev. Lett. **76**, 2290 (1996).
[19] A.G. Balanov, N.B. Janson and E. Schöll, Phys. Rev. E **71**, 016222 (2005).
[20] T. Shimada and T. Moriya, Prog. Theor. Exp. Phys. **2014**, 023A05 (2014).
[21] N. Chaubey, S. Mukherjee, A.N. Sekar Iyengar and A. Sen, Phys. Plasmas **22**, 022312 (2015).
[22] T. Fukuyama and M. Okugawa, Phys. Plasmas **24**, 032302 (2017).
[23] T. Fukuyama, K. Hagimine and R. Miyazaki, J. Phys. Soc. Jpn. **86**, 095003 (2017).
[24] N. Inaba, H. Ito, K. Shimizu and H. Hikawa, Prog. Theor. Exp. Phys. **2018**, 063A01 (2018).
[25] T. Fukuyama and M. Omoto, Prog. Theor. Exp. Phys. **2021**, 073J01 (2021).
[26] T. Fukuyama and N. Nishida, Plasma Fusion Res. **17**, 1201002 (2022).
[27] M. Novák, Czech. J. Phys. **10**, 954 (1960).
[28] N.L. Oleson and A.W. Cooper, Adv. Electron. Electron Phys. **24**, 155 (1968).
[29] K. Ohe and S. Takeda, Contrib. Plasma Phys. **14**, 55 (1974).
[30] I. Grabec and S. Mikac, Plasma Phys. **16**, 1155 (1974).
[31] N. Bekki, J. Phys. Soc. Jpn. **50**, 659 (1981).
[32] M. Rottmann and K.H. Spatschek, J. Plasma Phys. **60**, 215 (1998).
[33] L. Sirghi, K. Ohe and G. Popa, J. Phys. D: Appl. Phys. **31**, 551 (1998).
[34] See the following page. https://youtu.be/sTCUC9Vv8R8
[35] N.H. Packard, J.P. Crutchfield, J.D. Farmer and R.S. Shaw, Phys. Rev. Lett. **45**, 712 (1980).